Ultrafast Dynamics of Carrier Mobility in a Conjugated Polymer Probed at Molecular and Microscopic Length Scales

A. Devižis,[1] A. Serbenta,[1] K. Meerholz,[2] D. Hertel,[2,*] and V. Gulbinas[1,†]

[1]*Institute of Physics, Savanoriu 231, Vilnius, Lithuania*

[2]*Department of Chemistry, Physical Chemistry, University of Cologne, Luxemburgerstrasse 116, 50939 Cologne, Germany*

(Received 24 July 2008; published 10 July 2009)

We used time-resolved electric-field-induced second-harmonic generation to probe the charge-carrier-mobility dynamics in amorphous organic materials on an ultrafast time scale. We were able to show that the mobility in poly-spiro-bifluorene-co-benzothiadiazol decreases from 0.1 $cm^2/V\,s$ at 1 ps to 10^{-6} $cm^2/V\,s$ within 1 μs. We attribute this dramatic decrease to the relaxation of the charge carriers within the density of states, clearly demonstrating the impact of disorder on the nanoscale charge transport in amorphous semiconductors.

DOI: 10.1103/PhysRevLett.103.027404 PACS numbers: 78.66.Qn, 73.61.Ph, 78.47.J−

The charge carrier mobility is one of the most important properties of organic materials for their application in optoelectronics. Based on calculations of the charge transfer integrals in organic solids [1] and effective-mass calculations of charge carriers in conjugated polymers [2] a charge mobility as high as 1000 $cm^2/V\,s$ can be predicted under ideal conditions. The calculated effective carrier mass agrees with experimental results obtained in single crystalline polydiacetylenes [3]. Thus, it appears that high mobilities in organic solids might be feasible. This is further substantiated by recent studies of optical coherence in these materials [4]. Microwave conductivity measurements in a ladder-type polyphenylene (MeLPPP) have shown that the one-dimensional mobility is close to 600 $cm^2/V\,s$ [5]. By contrast, the average bulk mobility in amorphous organic semiconductors is orders of magnitude lower [6]. Apparently, the conventional mobility, which is commonly assumed constant in time, might not be sufficient to fully describe charge transport on the nano scale, such as in organic devices. From a fundamental perspective it is of high interest to gain an understanding whether charge transport on molecular scales and ultrafast times is limited by the same processes as macroscopic transport, i.e., by energetic and geometric disorder and trapping.

For instance, if one considers photogeneration of charges in organic solar cells, the impact of excess photoexcitation energy on the mobility is not taken into account. Instead, device models use steady-state mobilities [7,8]. Considering that the size of organic device structures ranges from almost molecular dimensions to micrometer length, it is a challenge to probe charge transport on vastly different time scales ranging from femtoseconds to seconds. Insight into mobility dynamics could improve charge transport models. However, currently it is not possible to probe the time-resolved charge carrier mobility in disordered organic materials on ultrafast time scales due to the lack of an appropriate experimental method.

In this Letter, we introduce a novel experimental method to study the charge carrier mobility on ultrafast time scales in organic films and devices. Our technique is based on time-resolved electric field-induced second harmonic generation (TREFISH). We demonstrate that combination of TREFISH with conventional time-of-flight (TOF) measurements in a single experiment enables us for the first time to probe charge transport from molecular to microscopic dimensions with picosecond time resolution. As a model compound, we investigate poly-spiro-bifluorene-co-benzothiadiazol (PSF-BT, inset Fig. 3) member of a class of copolymers used for highly efficient polymer LEDs [9]. We demonstrate that dispersion reduces the mobility from about 0.1 $cm^2/V\,s$ at 1 ps to its stationary value of about 10^{-6} $cm^2/V\,s$.

Electric field-induced second harmonic generation (EFISH) is commonly used for the determination of molecular hyperpolarizability [10,11]. A pump-probe version of the method has been applied to investigate the electric-field dynamics on interfaces of inorganic semiconductors [12]. Any process changing the electric-field distribution in the material will affect the measured *temporal* second harmonic generation (SHG) signal; thus, the SHG intensity can be considered a good probe for changes of the electric-field strength due to charge motion. This method is applicable to all π-conjugated organic materials, and its time resolution is only limited by the duration of optical excitation pulses.

The devices used for the investigation were 115 nm thick PSF-BT films sandwiched between indium-tin-oxide (ITO) and aluminum as electrodes. The experimental details are described in the supporting information [13]. In short, the experimental setup for TREFISH is based on an amplified femtosecond Ti-sapphire laser generating 130 fs pulses (810 nm) at 1 kHz repetition rate. Synchronously with the optical pulses, 10 μs voltage pulses were applied to the sample through the high resistor. To avoid charge carrier injection, the device was reversely biased (i.e. the

aluminum electrode was positively biased). The polymer film was excited with 460 nm laser pulses. The fundamental laser radiation at 810 nm was used to probe the SHG efficiency in the polymer film with variable time delay relative to the excitation pulse. Field-induced fluorescence quenching was investigated using time-correlated single-photon counting with about 30 ps time resolution.

The device used in our investigation forms a parallel-plate capacitor that is charged by the applied voltage. Upon optical excitation the photocurrent partly discharges the capacitor, reducing the electric field responsible for SHG. The time-resolved SHG intensity (I_{SHG}) caused by optical excitation at different applied voltages is shown in Fig. 1(a). SHG is observed with p-polarized probe light only since unlike s-polarized light, it has a nonzero component of the electric field parallel to the applied field. We found that I_{SHG} is proportional to the square of the electic field (supporting information [13]) and is independent of electric-field polarity—in agreement with expectations. Small electric-field variations ΔE can be estimated from

$$\Delta E = [(I_{\mathrm{SHG}}/I^0_{\mathrm{SHG}})^{1/2} - 1]E_0. \quad (1)$$

where E_0 is the applied field (corrected for the built-in potential caused by differences in work function of the two electrodes), I_{SHG} and I^0_{SHG} are the SHG intensities with and without excitation, respectively.

As was shown for MeLPPP [14] two components are responsible for the change of the electric field upon optical excitation: excitons [$\Delta E_{\mathrm{exc}}(t)$] and, charge carriers [$\Delta E_{\mathrm{CC}}(t)$]. When the change of the electric-field amplitude is small, i.e., $\Delta E \ll E_0$ the field kinetics can be expressed as

$$\Delta E(t) \approx \Delta E_{\mathrm{exc}}(t) + \Delta E_{\mathrm{CC}}(t) \approx -n_{\mathrm{exc}}(t)\Delta\alpha E_0/2\varepsilon\varepsilon_0 - n(t)el(t)/\varepsilon\varepsilon_0. \quad (2)$$

Here $n_{\mathrm{exc}}(t)$ and $n(t)$ are densities of excitons and charge carriers, respectively, $\Delta\alpha$ is the change of the polarizabiliy, ε_0 is the permittivity of free space, ε is the dielectric constant of PSF-BT ($\varepsilon \sim 3$), e is the elementary charge, and $l(t)$ is the average drift length of the photogenerated charge carriers in the direction of the electric field. On a picosecond time scale $l(t)$ corresponds to the electron-hole separation distance.

The charge-carrier term $\Delta E_{\mathrm{CC}}(t)$ does not explicitly distinguish between bound geminate charge pairs (oriented along the electric field) and free charge carriers. However, the difference is taken into account by considering the separation distance between positive and negative charges.

The exciton term $\Delta E_{\mathrm{exc}}(t)$ results from the change of the polarizability $\Delta\alpha$ of conjugated segments upon their excitation, causing the charge displacement of <1 nm at electric field of about 10^6 V/cm [14–16] (supporting information). We evaluated the exciton contribution to the field kinetics *independently* by measuring the fluorescence kinetics, which is proportional to $n_{\mathrm{exc}}(t)$. When a voltage of 2 V is applied, the fluorescence kinetics is very similar to the TREFISH kinetics (supporting information). Both signals decay within 150 ps (Fig. 1). This indicates that at low voltages the exciton contribution dominates. At higher voltages the exciton contribution increases proportionally to E_0 [Eq. (2)]. To obtain the charge-carrier contribution $\Delta E_{\mathrm{CC}}(t)$ to the field kinetics, $\Delta E_{\mathrm{exc}}(t)$ was subtracted from $\Delta E(t)$. Figure 1(b) shows the dynamics of $\Delta E_{\mathrm{exc}}(t)$ and $\Delta E_{\mathrm{CC}}(t)$. $\Delta E_{\mathrm{CC}}(t)$ dominates at times >50 ps emphasizing the dominant role of the carrier mobility for the electric-field kinetics.

In the following, we analyze $\Delta E_{\mathrm{CC}}(t)$ in order to obtain the carrier mobility μ. We calculate the integral photocurrent $I_{\mathrm{int}}(t) = \int_0^t I(t)dt$ from the charge-carrier contribution to the electric-field kinetics as $I_{\mathrm{int}}(t) = -\Delta E_{\mathrm{CC}}(t)dC$, where C is the device capacitance, and d is the sample thickness. At longer times $I_{\mathrm{int}}(t)$ is directly measured by TOF. The time-dependent $I_{\mathrm{int}}(t)$ obtained from TREFISH and TOF is shown in Fig. 2. The $I_{\mathrm{int}}(t)$ is used to obtain the carrier mobility via $\mu = [dI_{\mathrm{int}}(t)/dt]/n(t)AE$, where A is the illuminated sample area (supporting information).

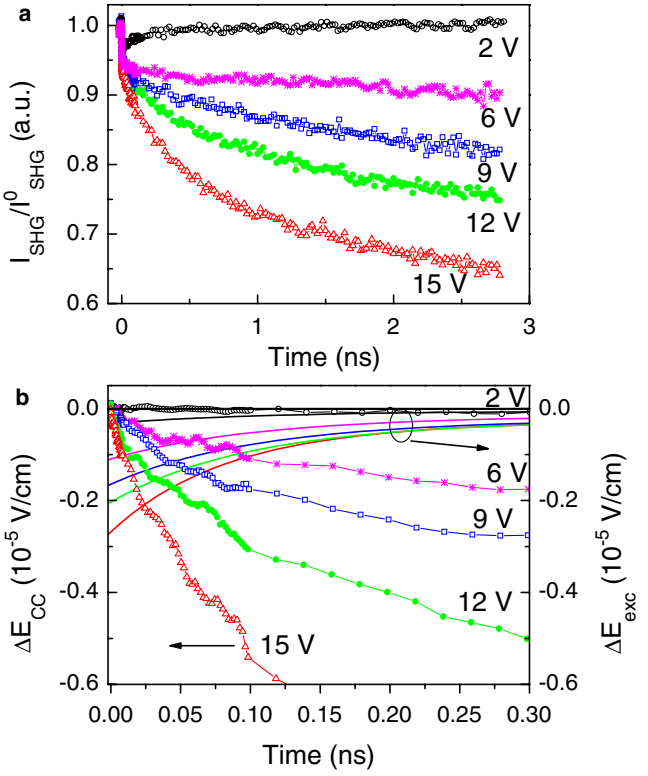

FIG. 1 (color online). (a) Excitation induced SHG intensity I_{SHG} kinetics at different applied voltages as indicated in the figure. (b) Electric-field kinetics [Eq. (2)] obtained from the I_{SHG} signal in (a) at early times. The symbols show the charge-carrier contribution $\Delta E_{\mathrm{CC}}(t)$ (left axis). The lines show the exciton contribution $\Delta E_{\mathrm{exc}}(t)$ (right axis) determined from the fluorescence kinetics (supporting information) from top to bottom: 2 V (black), 4 V (magenta), 9 V (blue), 12 V (green), 15 V (red).

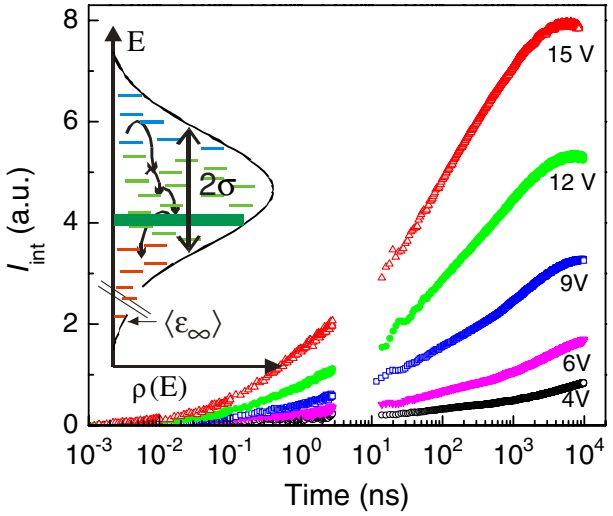

FIG. 2 (color online). Integrated photocurrent at different applied voltages (indicated in the figure) determined from TREFISH and TOF after subtraction of the exciton contribution $\Delta E_{exc}(t)$. The inset schematically depicts the relaxation of a charge carrier in the DOS of a disordered organic solid. The energy of transport sites is plotted as a function of density. The equilibrium carrier energy ε_∞ and transport energy (rectangular bar) are shown. The Gaussian DOS has a width of 2 times the disorder parameter σ.

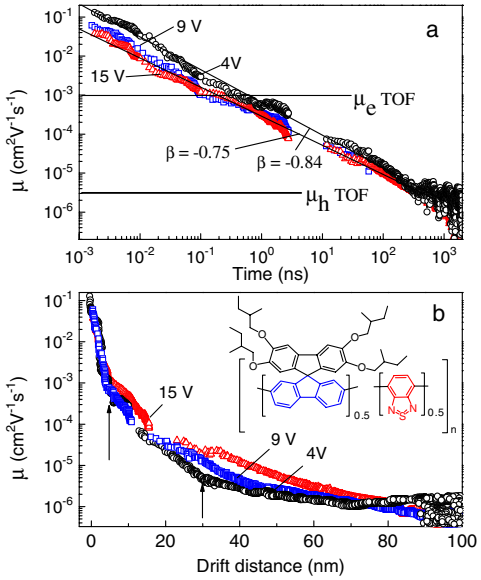

FIG. 3 (color online). (a) Carrier mobility kinetics in PSF-BT. The straight lines in (a) are fits to the data of 4 V and 15 V with slopes as indicated. The horizontal lines represent the electron and hole mobility as obtained from TOF measurements. (b) Dependence of the mobility on drift distance obtained as described in the text and supporting information. The arrows in (b) indicate different transport regimes as described in the text. The inset depicts the chemical structure of PSF-BT. For clarity only data for applied voltages of 4 V (black circles), 9 V (blue squares), and 15 V (red triangles) are shown.

In order to complete the analysis, the time-dependent charge-carrier density, $n(t)$, should be estimated. This density changes due to carrier generation from field-induced exciton dissociation and charge-carrier discharge at the electrodes. To obtain the generation rate we used the field-induced fluorescence quenching method assuming the number of generated carriers is proportional to the number of quenched excitons [17,18]. Finally, we estimate the decrease in charge-carrier concentration due to discharging at the electrodes by numerically solving the carrier motion equation. Details of the data analysis are given in the supporting information.

The time dependence of the carrier mobility $\mu(t)$ obtained from $I_{int}(t)$ is shown in Fig. 3(a). The mobility decreases by about 5 orders of magnitude from 0.1 $cm^2/V\,s$ at 1 ps to about 10^{-6} $cm^2/V\,s$ at hundreds of nanoseconds. The kinetics follow a power law $\mu \propto t^{-\beta}$ with β ranging from about 0.84 at low voltages to 0.75 at high voltages. A power law is typical for dynamic processes in amorphous organic materials. It is considered evidence that the mobility is limited by energetic and geometric disorder. The degree of dispersion depends on the energetic disorder characterized by the width σ of the density of states (DOS) [19–21]. Thus, disorder seems to control charge transport already on very short (picosecond) times. The decreasing slope of the mobility with increasing electric field can be rationalized as follows. We assume the electrostatic energy gain for a carrier jump of in an electric field of 10^6 V/cm is about 0.2 eV. This is a factor of 2 higher compared with a typical energetic disorder of about 80–120 meV for conjugated polymers [6]. Thus the disorder is effectively reduced with increasing the voltage from 4 to 15 V. The electric-field effect supports the view that on nanoscale transport the influence of temperature is expected to be negligible ($kT \sim 25$ meV). A dispersive mobility is in qualitative agreement with the Gaussian disorder model [6] and Monte Carlo simulations of the transient photocurrent, which are able to reproduce the experimental photocurrent on ns time scale [22]. However, to reproduce the dispersion also at ps times by MC simulation it is necessary to consider a fast on-chain mobility as will be described in detail in a forthcoming publication [22].

The high experimental mobility at early times corresponds to both, the mobility of holes and electrons, since both are of similar magnitude at least at molecular distances [1]. Initially, the electron-hole separation distance increases during the relaxation within the DOS (inset Fig. 2). Later, it evolves into macroscopic drift characterized by trapping or detrapping events [19]. From TOF measurements on thick devices (supporting information) we determined steady-state mobilities of $\sim 10^{-3}$ $cm^2/V\,s$ and $\sim 10^{-6}$ $cm^2/V\,s$ for electrons and holes, respectively. The relatively high electron mobility is in agreement with measurements on a related polymer [23].

We can conclude that at short times (<1 ns) the mobility in PSF-BT is determined by electrons. At submicrosecond

times, when the average drift distance reaches 30 to 50 nm and most of the faster moving electrons are already extracted from the device, the mobility is attributed to the slower moving holes.

Comparing our results to the mobility of 600 $cm^2/V\,s$ recently reported for MeLPPP [5] in dilute *solution*, we note that this value is the time-average for 1-dimensional motion along a few repeat units of the polymer chains only and, therefore, its relevance for understanding processes in actual devices is limited. Using TREFISH we obtained a *time-resolved* mobility in device structures that are commonly used for organic LEDs or solar cells. The mobility determined in our study corresponds to the carrier motion perpendicularly to the device normal. We were able to follow the time dependence of the mobility in the entire time domain relevant to such devices. This is more evident by translating the temporal dependence of the mobility into a spatial dependence (supporting information). Figure 3(b) shows the carrier mobility expressed as a function of the average drift distance. The carriers drift about 5 nm (during 100 ps) with high, but rapidly decreasing mobility (10^{-1}–10^{-3} $cm^2/V\,s$). Between 5 and 30 nm the mobility is 10^{-3}–10^{-5} $cm^2/V\,s$. After about 30–50 nm, the mobility reaches a stationary value of 10^{-6} $cm^2/V\,s$. Apparently, there are three distinct transport regimes related to transport along a conjugated segment, hopping within the density of states and steady-state transport in equilibrium. An in-depth study on these mobility phases will be the subject of a forthcoming publication [22].

In conclusion, we demonstrated that TREFISH is a very powerful tool for the investigation of the carrier drift in organic materials on ultrafast time scale. This technique yields essential transport properties for the development of theoretical models of nanoscale molecular devices when the macroscopic mobility is not an adequate parameter. The combination of TREFISH and TOF enabled us to evaluate the charge-carrier-mobility dynamics from ps to μs time scales. In particular, our results demonstrate that the excess energy introduced into the system upon photogeneration can be converted into a very high initial carrier mobility. Later this energy is thermally dissipated, and as a result, the mobility decreases. It is apparent that taking into account a time-dependent mobility will improve current models for organic solar cells [7,8]. It might also be important for future electrically driven organic lasers [24], where charge transport takes places at high electric fields, and the relaxation of charge carriers within the DOS is expected to proceed on a ps time scale.

We would like to acknowledge Merck KGaA for providing the PSF-BT. We thank the Lithuanian State Science and Studies Foundation, Deutsche Forschungsgemeinschaft (DFG), and Fonds der Chemischen Industrie (FCI) for financial support.

*dirk.hertel@uni-koeln.de
†vidgulb@ktl.mii.lt

[1] V. Coropceanu, J. Cornil, D. A. da Silva Filho, Y. Olivier, R. Silbey, and J.-L. Bredas, Chem. Rev. **107**, 926 (2007).
[2] J. W. van der Horst, P. A. Bobbert, M. A. J. Michels, and H. Bässler, J. Chem. Phys. **114**, 6950 (2001).
[3] A. Horvath, G. Weiser, C. Lapersonne-Meyer, M. Schott, and S. Spagnoli, Phys. Rev. B **53**, 13 507 (1996).
[4] F. Dubin, R. Melet, T. Barisien, R. Grousson, L. Legrand, M. Schott, and V. Voliotis, Nature Phys. **2**, 32 (2006).
[5] P. Prins, F. C. Grozema, J. M. Schins, S. Patil, U. Scherf, and L. D. A. Siebbeles, Phys. Rev. Lett. **96**, 146601 (2006).
[6] for a recent review see, D. Hertel and H. Bässler, Chem. Phys. Chem. **9**, 666 (2008).
[7] V. D. Mihailetchi, J. Wildeman, and P. W. M. Blom, Phys. Rev. Lett. **94**, 126602 (2005).
[8] V. D. Mihailetchi, L. J. A. Koster, J. C. Hummelen, Wildeman, and P. W. M. Blom, Phys. Rev. Lett. **93**, 216601 (2004).
[9] D. C. Müller, A. Falcou, N. Reckefuss, M. Rohjan, V. Wiederhirn, P. Rudati, H. Frohne, O. Nuyken, H. Becker, and K. Meerholz, Nature (London) **421**, 829 (2003).
[10] Ch. Bosshard, G. Knöpfle, P. Pretre, and P. Günter, J. Appl. Phys. **71**, 1594 (1992).
[11] J. W. Perry, in *Nonlinear Optical-Properties of Molecules and Materials, in Materials for Nonlinear Optics*, edited by S. R. Marder, E. J. Sohn, and G. D. Stucky (American Chemical Society, Washington, D.C., 1991), p. 67.
[12] Y. D. Glinka, T. V. Shahbazyan, I. E. Perakis, N. H. Tolk, X. Liu, Y. Sasaki, and J. K. Furdyna, Appl. Phys. Lett. **81**, 3717 (2002).
[13] See EPAPS Document No. E-PRLTAO-103-022930 for supporting information. For more information on EPAPS, see http://www.aip.org/pubservs/epaps.html.
[14] V. Gulbinas, Y. Zaushitsyn, V. Sundström, D. Hertel, H. Bässler, and A. Yartsev, Phys. Rev. Lett. **89**, 107401 (2002).
[15] V. Gulbinas, R. Kananavicius, L. Valkunas, and H. Bässler, Phys. Rev. B **66**, 233203 (2002).
[16] M. G. Harrison, S. Möller, G. Weiser, G. Urbasch, R. F. Mahrt, H. Bässler, and U. Scherf, Phys. Rev. B **60**, 8650 (1999).
[17] D. Hertel, E. V. Soh, H. Bässler, and L. J. Rothberg, Chem. Phys. Lett. **361**, 99 (2002).
[18] W. Graupner, G. Cerullo, G. Lanzani, M. Nisoli, E. J. W. List, G. Leising, and S. De Silvestri, Phys. Rev. Lett. **81**, 3259 (1998).
[19] I. I. Fishchuk, A. Kadashchuk, H. Bässler, and S. Nespurek, Phys. Rev. B **67**, 224303 (2003).
[20] S. C. J. Meskers, J. Hübner, M. Oestreich, and H. Bässler, J. Phys. Chem. **105**, 9139 (2001).
[21] C. Rothe and A. P. Monkman, Phys. Rev. B **68**, 075208 (2003).
[22] A. Devizis, D. Hertel, and V. Gulbinas (to be published).
[23] L. L. Chua, J. Zaumseil, J. F. Chang, E. C. W. Ou, P. K. H. Ho, H. Sirringhaus, and R. H. Friend, Nature (London) **434**, 194 (2005).
[24] B. K. Yap, R. D. Xia, M. Campoy-Quiles, P. N. Stavrinou, and D. D. C. Bradley, Nature Mater. **7**, 376 (2008).